A Method to Recognize 3D Shapes of Moving Targets based on Integration of Inclined 2D Range Scans

Tetsushi Ikeda, Yoshihiro Chigodo, Takahiro Miyashita, Fumio Kishino, and Norihiro Hagita

***Abstract*— Recently, laser-based people-tracking systems have received increasing attention for their ability to localize human subjects precisely in crowded situations. However, in a real environment, there exist many kinds of moving objects other than people, and previous methods have focused only on humans. To design a more sophisticated system, it is necessary to distinguish humans from observed objects and recognize their individual condition—for example, the kind and amount of belongings they are carrying. However, in previous methods using 2D laser range finders (LRFs), it proved difficult to recognize the type of target since all sensors observe a common horizontal plane and only the 2D contours of their targets. In this study, to recognize the type of target, we observe the 3D shapes of objects moving in their environment by installing LRFs with an angle of inclination. So far, in the area of 3D modeling, LRFs have been used to construct 3D models of static objects by moving the sensor and registering multiple views. In contrast, our method observes moving objects by using a static LRF network in the environment. Experimental results are shown to confirm the effectiveness of the proposed method.**

I. Introduction

UNDERSTANDING how people behave in public spaces is a key challenge in the design of intelligent environments that provide condition-related services to those people. Many kinds of people-recognizing sensors have been tested in research projects [1-4] that aim to produce such a system. Much work has also been done in the area of computer vision systems [5] that can locate people and understand their behavior. One advantage of using cameras, for example, is that we can make use of a variety of information such as colors and motion gestures. At the same time, the use of cameras is limited by privacy issues. Furthermore, they are affected by changes in lighting conditions. For example, it is sometimes difficult to use them in a shopping mall that is illuminated by sunlight streaming through the windows.

Recently, laser range finders (LRFs) that scan a 2D plane have been much used as a tool for locating people in "smart" environments. Since the size and price of these devices have decreased, it is now more feasible to install LRFs in different types of public environment and use them to provide services. Furthermore, LRFs are robust against changes in light conditions, and there are no serious privacy issues that limit their use.

Manuscript received September 15, 2010. This research was supported by the Ministry of Internal Affairs and Communications of Japan.

Tetsushi Ikeda, Takahiro Miyashita and Norihiro Hagita are with ATR-IRC Laboratories, Kyoto 619-0288, Japan. E-mail: ikeda@atr.jp.

Yoshihiro Chigodo and Fumio Kishino are with the Department of Multimedia Engineering, Graduate School of Information Science and Technology, Osaka University, Osaka 565-0871, Japan.

So far, LRFs have been used to detect people. Arras et al. [6] used a LRF mounted 30 cm above the floor and detected people using boosted features. Luber et al. [7] also used a LRF at a height of 15 cm above the ground and proposed a state transition model to represent time-varying appearances of objects. Since they observe target at a fixed height, it is difficult to classify many kinds of object with various shapes.

LRFs have been successfully used to track people in a crowded environment. In one study, Cui et al. [8] used LRFs to track a large number of people. Glas et al. [9] placed LRFs in a shopping mall to predict the trajectory of walking subjects. Previous methods that observe people using LRFs have mainly focused only on estimating the location of people. To estimate location and recognize posture as well, Matsumoto et al. [10] used a kinematic model of the human body. But their targets are limited to humans.

In a real shopping mall, there exist not only people but many kinds of objects, such as baggage, shopping carts, and cardboard boxes. Therefore, for intelligent systems that provide services to targets, it is necessary not only to locate the targets, but to recognize the type of target correctly. The limitation of previous methods using LRFs is that they only observe the 2D contours of a target. They position LRFs to observe a horizontal plane.

Layered LRFs are used to observe 3D representation of targets. Mozos et al. [11] proposed a person detection system by voting detection results from multiple LRFs in different height. Gidel et al. [12] also used four LRFs that are located in 4 layer planes. However, their methods have mainly focused only on detection and estimation of people and do not classify many kinds of objects.

Recently, Spinnelo et al. [13] applied a 3D LRF that is composed of 64 planer LRFs and observes 3D shape of objects in 10Hz. 3D LRFs are promising approach to detect and classify the target. They successfully detected people by integrating multiple classifiers based on voting.

In this paper, we propose a simple method that uses 3D shape information to recognize the type of target while still using the same facilities as previous laser-based tracking methods. We install LRFs in an environment with an angle of inclination and observe the 3D shapes of targets as they move through that environment. Previous 3D modeling methods observed static targets using a moving LRF [14-17] or a 3D scan LRF [13]. Our method, however, observes moving targets using static LRFs. Although the observed shapes are not as precise as those observed with previous 3D shape modeling methods, it is useful to distinguish several types of

target in an environment. We have confirmed that our method can recognize walking humans, moving solid objects, and a combination of these targets.

The rest of this paper is organized as follows. First, we explain a method of observing the 3D position and shape of a target. Then we present the results of an experimental evaluation of our prototype system. Finally, we discuss the proposed approach and offer a conclusion.

II. Estimating 3D Shapes using 2D Scan LRFs in Environments

In our method, we first estimate the 2D position of targets using LRFs that observe a horizontal plane ("horizontal LRFs"). Then, for each detected target, we observe contours using LRFs that scan inclined planes ("inclined LRFs"), and construct a 3D shape representation. By matching the observed shape and trained 3D model of objects on the basis of target orientation, we obtain the type of target.

By using inclined LRFs that are fixed in the environment, a target is only observed at around a certain height that depends on the position of the target, and the range of observation is quite limited. If a target goes across the sensing area, a 2D range scan LRF can observe the 3D shape of the target by integrating observations (Figure 1). In our method, a sequence of observed contours using 2D range scans is accumulated by aligning the centers of observed contours. Finally, a 3D shape is obtained by integrating observations from all the LRFs, and represented in a grid model indexed by height and angle.

Compared to previous 3D modeling methods using LRFs, which assume that targets do not move, the 3D observations we obtained are not very precise. Firstly, the observation range of a target is limited and depends on the moving trajectory. Secondly, targets such as humans change their shape when they walk. Thirdly, the orientation of a target may change during observation.

The first problem depends on the placement of sensors in the environment. We further discuss this problem in section IV. For the second problem, we introduce a 3D shape model that represents radial distances and variances. For the third problem, we adopt an greedy search method based on shape matching, where current orientation of a target is estimated so that the integrated 3D shape is the most similar to the model.

A. Estimating 2D position of targets

First we estimate positions of targets by using LRFs that observe the shared horizontal plane. The height of the plane is set to 85 cm in the experiment. At this height, people are observed at the waist and their shapes do not change much as they walk.

To track the positions of all targets in the environment, we applied the method proposed in [9]. First, a background model is computed for each sensor by analyzing hundreds of scan frames to filter out noise and moving objects. Points detected in front of this background scan are grouped into contour features within a certain size range persisting over several scans. Each person is segmented as a blob of contours and the center is computed for each blob. Figure 2 shows an example of the observed contour of a person.

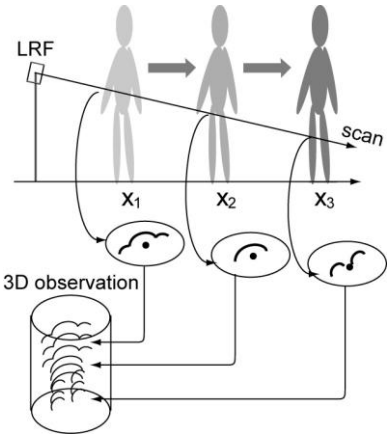

Figure 1. Estimating 3D shape of moving targets by integrating observations with inclined 2D range scan. A sequence of observations are aligned based on the centers of the observations.

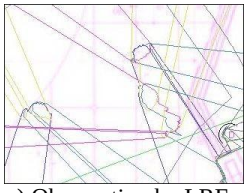

a) Observation by LRFs

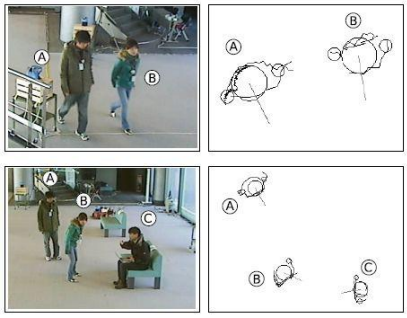

b) Examples of scenes and estimated positions. Circles show the detected body and arms.

Figure 2. Estimating position of human subjects with 2D horizontal scan LRFs.

B. Estimating 2D contours of targets by observing a inclined plane

When a 2D range scan LRF is placed with its scan plane inclined from the horizontal plane, the position of each point of observed contours P in the sensor coordinate are rotated to compute the position in 3D space P' (Figure 3(a)), where S is the position of the sensor and $\mathbf{n}$ is a unit vector parallel to the axis of the rotation of the sensor. We assume the rotation vector $\mathbf{n}$ is parallel to the horizontal plane. In vector form, the rotated vector $\mathbf{x}' = \mathrm{SP}'$ is computed from a vector $\mathbf{x} = \mathrm{SP}$ on the ground plane as follows:

$$\mathbf{u} = \mathbf{x} - (\mathbf{x}\cdot\mathbf{n})\mathbf{n},$$
$$\mathbf{v} = \mathbf{n}\times\mathbf{u}, \qquad (1)$$
$$\mathbf{x}' = (\mathbf{x}\cdot\mathbf{n})\mathbf{n} + \mathbf{u}\cos\alpha + \mathbf{v}\sin\alpha,$$

where α is the angle of rotation [see Figure 2(b)]. Then Eq. (1) is represented using a rotation matrix:

$$\mathbf{x}' = \mathbf{R}(\mathbf{n},\alpha)\mathbf{x},$$

$$\mathbf{R}(\mathbf{n},\alpha) = \cos\theta\,\mathbf{I}_3 + (1-\cos\alpha)\mathbf{n}^t\mathbf{n} + \sin\alpha[\mathbf{n}]_\times,$$

$$[\mathbf{n}]_\times \equiv \begin{bmatrix} 0 & -n_z & n_y \\ n_z & 0 & -n_x \\ -n_y & n_x & 0 \end{bmatrix}, \qquad (2)$$

where $\mathbf{I}_3$ is a 3x3 identity matrix and the elements of vector $\mathbf{n}$ are defined as $\mathbf{n} = (n_x, n_y, n_z)$.

After this rotation process, positions of all contour features are translated into the global coordinate. We assume the positions and directions of LRFs are calibrated in advance.

C. Integrating 3D Shape of Moving Targets

At each time, for each detected blob of contours, we compute the center of the contours observed by horizontal LRFs (Figure 4(a)):

$$\bar{\mathbf{x}} = \sum_k \mathbf{x}_k / N,$$

where k is a index of points, and N is the number of points in the blob.

Based on the computed center of each target, we compute radial distance from the center and the angle in a horizontal plane. Figure 4 (b) shows a computed radial distance at a height. After observing a sequence of observed contours, we have a set of radial distances (Figure 4 (c)). To cope with changing shapes of targets, we compute the variance of distances in each grid of the angle (Figure 4 (d)). Finally, the average and the variance and the total number of data to compute these statistics at height h and angle θ are stored in a model M_{ij}, where i, j are indexes of height and angle of the model:

$$i = \lfloor h/\Delta_h \rfloor,$$
$$j = \lfloor \theta/\Delta_\theta \rfloor,$$

Δ_θ is the grid size of angle, Δ_h is the grid size of height. We represent a 3D shape of a target by a set of models and describe the 3D model as $\mathbf{M} = \{M_{ij}\}$

For each type of targets, we construct a 3D shape model $\mathbf{M}$. In the training stage, we assume the orientations of targets are known. After aligning observed contours, radial distances in a sequence of training data are integrated to a shape model.

These statistics are an effective aid for coping with changes of shape. The inverse of the variance represents confidence of representation and is considered in the recognition stage.

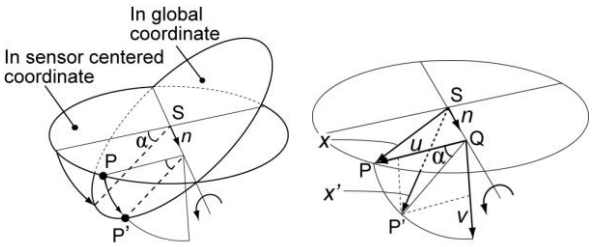

a) Rotation of scan plane. b) Computation of x'.

Figure 3. Computing positions of observed contours by rotating 2D scan.

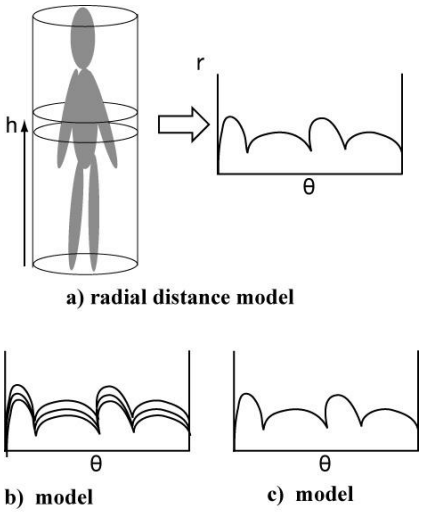

Figure 4. 3D grid model.

D. Measuring Distance between 3D Shapes

To match the 3D contour of a current observation and the constructed models, a distance measure is defined. Suppose an observed 3D shape is in grid representation $\mathbf{Z}$. The distance between observation and 3D shape model $\mathbf{M}$ is defined as follows.

First we compute normalized distance D_{ij} as

$$D_{ij} = \frac{|\,\mathrm{avg}(Z_{ij}) - \mathrm{avg}(M_{ij})\,|}{\sqrt{\mathrm{var}(M_{ij})}},$$

where $\mathrm{avg}(M_{ij}), \mathrm{var}(M_{ij})$ are average and variance stored in the model M_{ij}.

Then the distance is computed as

$$\text{distance}(\mathbf{Z},\mathbf{M}) = \sum_{i,j} f_{ij} / N, \qquad (3)$$

$$f_{ij} = \begin{cases} 0 & \text{if number of data} = 0 \text{ in } Z_{ij} \text{ or } M_{ij} \\ R_{\max} & D_{ij} > R_{\max} \\ D_{ij} & \text{otherwise} \end{cases},$$

where N is the effective number of index (i, j) that both number of data for Z_{ij} and M_{ij} is larger than one. When N is 0, distance $(\mathbf{Z},\mathbf{M})$ is set to infinity. To improve the robustness against noise, we introduce threshold $R_{\max}$.

Note that Eq. (3) is computed between a sequence of 3D shapes and a trained model. As the target moves further and more observations are accumulated, the computed distance reflects contours of larger parts of the object.

E. Estimating Orientation and Type of Target with a Greedy Search

To estimate the type of objects detected, the 3D shape model is matched to each detected trajectory of an object. However, the orientations of a target at each time step are required to compute the distance measure.

A simple method to estimate the orientation of a target is computing the direction of motion from several frames. However, estimated directions are noisy if we use smaller number of frames, and do not correct if we use larger number of frames. It was quite difficult to estimate the orientation when a target stopped and turned the direction. These result motivated us to apply an estimation method based on the shape matching.

We apply a greedy search method to search the sequence of target orientations and minimize the distance measure in (time, orientation) space. Figure 5 shows a computation step.

We compute 3D shape $\mathbf{Z}(\tau,k)$ at each step τ and orientation indexed by k. First, $\mathbf{Z}$ is initialized to empty for $\tau = 0$. At each time step, $\mathbf{Z}(\tau,k)$ is computed by adding observation $\mathbf{O}(\tau)$ at time τ to a shape $\mathbf{Z}$ at the previous time step while permitting a small amount of rotation $\theta = k\Delta_\theta$:

$$\mathbf{Z}(0,k) = \text{empty}(\text{all } Z_{ij} \text{ have no data}) \text{ for all k},$$

$$\mathbf{Z}(\tau,k) = \min_k \left[\text{distance}\left(R_\theta[\mathbf{Z}(\tau-1,k+l)] + \mathbf{O}(\tau), \mathbf{M}\right) \right], \qquad (4)$$

$$-\frac{\theta_{\max}}{\Delta_\theta} \le l \le \frac{\theta_{\max}}{\Delta_\theta},$$

where $R_\theta[\cdot]$ is the rotation operator along the vertical axis by

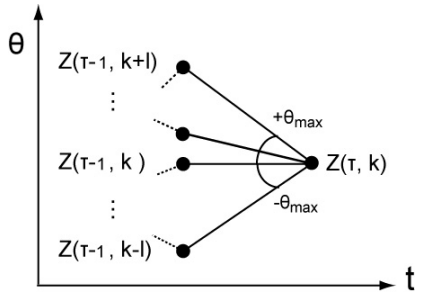

Figure 5. Estimating type of target with dynamic programming.

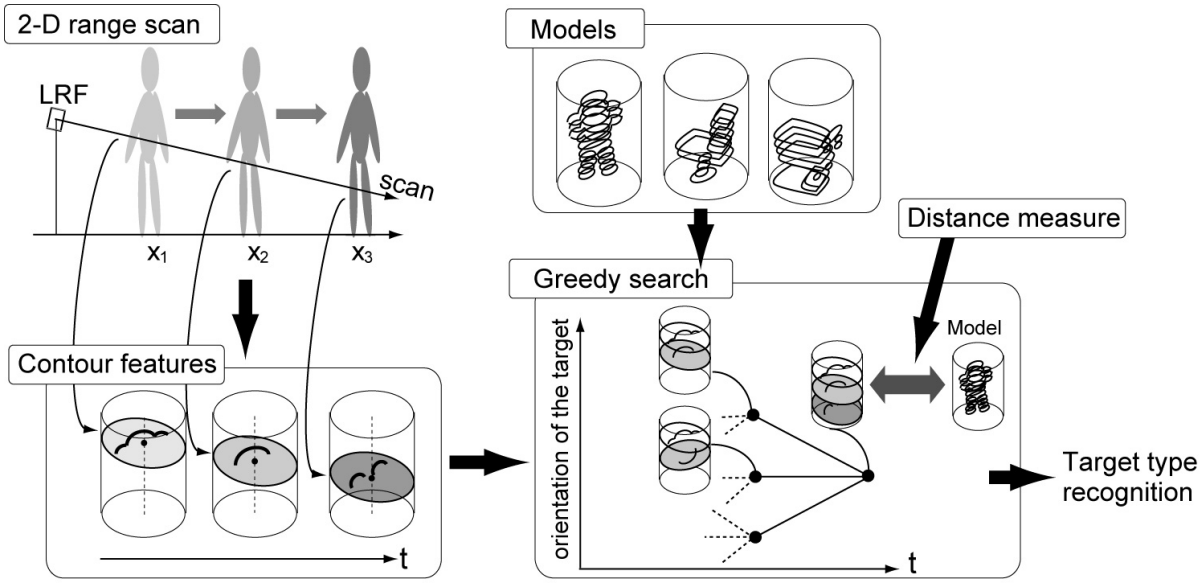

Figure 6. System overview.

θ , and $\theta_{\max}$ is a fixed parameter that limits motions of targets.

To compute the cost of matching the model at time t,

$$\text{cost}(t) = \min_k \mathbf{Z}(t,k). \quad (5)$$

By applying this process to all objects of type c, and selecting the type that minimizes the cost function, we estimate the type of target:

$$c^* = \arg\min_c \{\text{cost}_c(\tau)\}, \quad (6)$$

where $\text{cost}_c(\tau)$ is the estimated minimum cost of object type c. We can also estimate a sequence of target orientations that minimizes the cost function.

Figure 6 summarizes the proposed algorithm to estimate positions and classify types of objects based on 3D shape.

We would emphasize an important point in our approach: although the observed 3D shapes are not perfect, it is still possible to discriminate several types of targets while still using the same facilities as previous tracking methods that rely on 2D range sensors in the environment.

III. EXPERIMENTS

A. Experimental Setup

We conducted experiments in a 5-m-radius area (Figure 7). People and objects in this area were monitored using 14 LRFs mounted at a height of 85 cm (Figure 8). Six LRFs observed a horizontal plane at the 85 cm height and eight LRFs were inclined by 10 degrees from the horizontal plane. We selected the angle so that about half of a person's shape is scanned by one LRF as the person walks 5 meters. Currently we have confirmed the effects of integrating more than two inclined LRFs in offline experiments.

Table 9 shows the types of objects recorded and Figure 10 shows examples of the 3D models obtained. To evaluate the applicability of the proposed method, we used human subjects, solid objects like carts and baggage, and a combination of the two for experimental targets. We consider the combination of humans and objects as a new, different type of target. Together, they represent typical targets that exist in real shopping mall environments.

First we recorded data for the training stage. We recorded each target moving on a straight line for around 30 seconds. Then for the testing stage, we recorded each target moving around for a few minutes. We picked up 10 sequences for each 11 detailed target type in Table 9.

We used $\theta_{\max}$ = 10 [degree] to cover all trajectories of targets in the experimental data. We used $R_{\max}$ = 5 to suppress the effects of large noise, which means a data point that is larger than 5 sigma is considered as noise and ignored. We use Δ_h = 20 [cm], Δ_θ = 2 [degree] if these values are not specified explicitly.

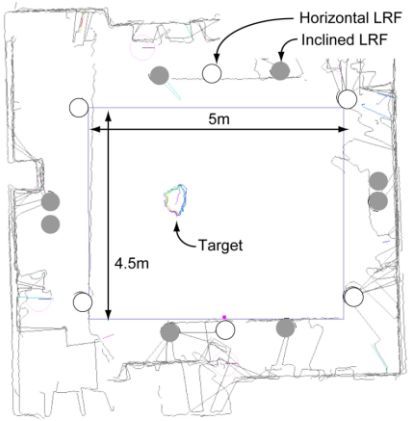

a) Placement of LRFs. Surrounding lines are background observation when there are no objects around the center of this environment.

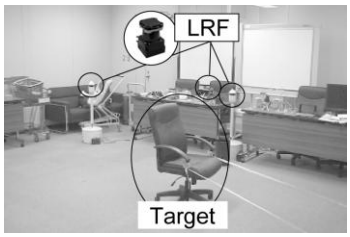

b) Example of constructing a model of a chair.

Figure 7. Experimental environments.

Specifications	
Product name	UTM-30LX (HOKUYO AUTOMATIC)
Detection range	0.1 to 30[m], 270 [degree]
Accuracy	30mm (0.1 to 10m)
Angular resolution	0.25 [degree]
Scan time	25 [msec/scan]

Figure 8. The laser range finder used.

Table 9. Types of target. A person carrying an object is categorized as a different type of target.

Index	Type	Detailed type
P1	person	with nothing
P2		with a backpack
P3		with a shoulder bag
P4		carrying a suitcase
O1	object	chair
O2		baby car
O3		shopping cart
O4		cardboard box
PO1	person+object	pushing a baby car
PO2		pushing a shopping cart
PO3		pushing a hand truck with cardboard box

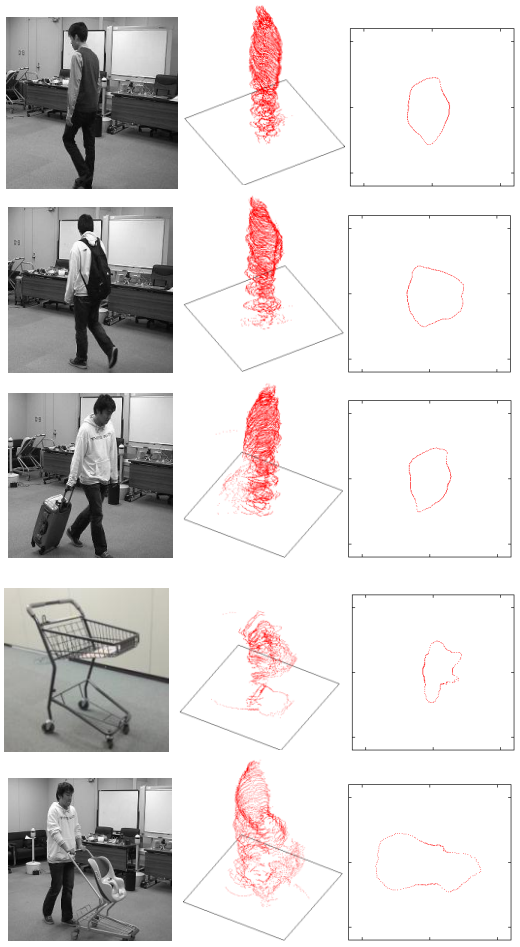

Figure 10. Examples of employed targets, 3D shape, and 2D contours. From top to bottom: Person, person with a backpack, person carrying a suitcase, shopping cart, person pushing a baby car. It is difficult to distinguish these targets only by the 2D contours. The 3D shape have much information to distinguish them.

B. *Classification Evaluation*

Table 11 summarizes the rate of correct classification. For this evaluation, testing samples contains 110 samples for each detailed type. Table 11(a) shows the average precision of the proposed method compared to the results obtained when only LRFs that scan a horizontal plane are used and the results when fixed averaged variance is used in distance measure in Eq.(3). By using 3D shape observation, the classification rate becomes better. Table 11(b) shows the changes of the results for different resolution of the shape model.

Figure 12 shows the confusion matrix for classifying the detailed type. We can see that the recognition failure occurs only among detailed classes in the same type. For example, person with a small object is sometimes estimated as a person with a different small object, but not as a target in different types. The precision of recognizing the type in Table 9 is 100 %.

Table 11. Rate of correct classification

a) Rate of correct classification of the detailed types for 110 testing data.

Method	Precision [%]
2D contours matching	36.4
3D shape matching using fixed variance	70.9
3D shape matching considering variance	74.5

b) Precision for different resolutions of the model.

Δ_h [mm]	Δ_θ [degree]	Precision [%]
20	2	74.5
50	5	74.5
100	10	74.5
150	50	68.2
200	20	63.6

IV. Discussion

A. *Placement of LRFs*

First, since the observation height depends on the location of LRFs in their environments, only limited ranges of a target may be observed. If it is possible to analyze the flow of people and objects in advance, the targets are scanned effectively by arranging LRFs carefully. We plan to estimate the best arrangement of sensors on the basis of observed trajectories.

However, this kind of partial observation is a fundamental problem in our method. When we apply this method to a real shopping mall environment, we want the system to recognize the large category quickly. So constructing a classification tree is useful, as it returns the large category of a target when observations are not enough and gradually returns detailed information on the type of target.

B. *Problem of Changing Shapes*

To cope with changes of shape during observation, we introduce a distance measure that considers the variance of radial distances in training data. For example, in constructing a 3D shape model of a walking person, we must factor how the contours of the legs are changing. If a simple average of the observed radial distances is used for constructing models, the 3D shape is blurred and does not match a real human shape. To cope with this problem, we consider the variance of radial distances to the proposed distance function. When the quantity of training data is not enough (less than 8), we have used a total average variance instead. In Table 11(a), the rate of correct classification improved by using the distance function that consider the variance.

C. *Resolution of 3D Model*

Table 11(b) shows how the results change when we adopt different parameters. In this experiment, using

parameters Δ_h = 100 [mm], Δ_θ = 10 [degree] results in relatively good precision with smaller computation cost. The quality of the resolution depends on the targets and their environment.

V. CONCLUSION

In this study, we proposed a simple method that not only estimates the position of targets in their environment but recognizes the type of target using the same facilities as previous laser-based tracking methods. By installing LRFs with an inclination from the horizontal plane and observing the 3D shapes of moving targets, our method can estimate the type of target.

To provide services in a real shopping mall environment where many kinds of target exist, it is important to recognize whether the target is a human subject or an object of some kind. Moreover, in working towards a system that can return good results in public spaces where people carry many forms of baggage, the proposed method provides useful cues.

Experimental results show the effectiveness of the proposed method. Our future plan includes testing the method in real shopping mall environments.

actual type

estimated type	person				object				person+object		
	P1	P2	P3	P4	O1	O2	O3	O4	PO1	PO2	PO3
P1	50										
P2	40	90	20	10							
P3	10	10	50	40							
P4			30	50							
O1					60						
O2					30	100					
O3					10		100				
O4								100			
PO1									100	40	
PO2										50	
PO3										10	100

Figure 12. Confusion matrix of classifying the detailed type [%]. Each row of the matrix represents a estimated type, while each column represents an actual type.

REFERENCES

[1] A. Pentland, "Smart rooms," *Scientific American*, 274-4, 68/76, 1996.

[2] R. A. Brooks, "The intelligent room project," *Proc. 2nd Int. Cognitive Technology Conf.*, 1997.

[3] C. D. Kidd, R. J. Orr, G. D. Abowd, C. G. Atkeson, I. A. Essa, B. MacIntyre, E. Mynatt, T. E. Starner and W. Newstetter, "The aware home: A living laboratory for ubiquitous computing research," *Proc. Int. Workshop on Cooperative Buildings (CoBuild '99)*, 1999, pp. 191-198.

[4] T. Mori, H. Noguchi, A. Takeda, T. Sato, "Sensing room: Distributed sensor environment for measurement of human daily behavior," *Int. Conf. on Networked Sensing Systems*, 2004, pp. 40─43.

[5] T. B. Moeslund, A. Hilton, V. Krüger, "A survey of advances in vision-based human motion capture and analysis," *Computer Vision and Image Understanding*, Vol. 103, No. 2-3, 2006, pp. 90─126.

[6] K. O. Arras, O. M. Mozos, W. Burgard, "Using Boosted Features for the Detection of People in 2D Range Data", *Proc. IEEE Int. Conf. on Robotics and Automation (ICRA)*, 2007.

[7] M. Luber, K. O. Arras, C. Plagemann, and W. Burgard, "Classifying Dynamic Objects," *Autonomous Robots*, Vol. 26, No. 2-3, 2009, pp. 141-151.

[8] J. Cui, H. Zha, H. Zhao, and R. Shibasaki., "Laser-based detection and tracking of multiple people in crowds," *Computer Vision and Image Understanding*, Vol. 106, No. 2-3, 2007, pp. 300–312.

[9] D. F. Glas, T. Miyashita, H. Ishiguro, and N. Hagita, "Laser-Based Tracking of Human Position and Orientation Using Parametric Shape Modeling," *Advanced Robotics*, Vol. 23, No. 4, 2009, pp. 405-428.

[10] T. Matsumoto, M. Shimosaka, H. Noguchi, T. Sato and T. Mori, "Pose estimation of multiple people using contour features from multiple laser range finders," *Proc. Int. Conf. on Intelligent Robots and Systems (IROS)*, 2009, pp. 2190-2196.

[11] O. M. Mozos, R. Kurazume, T. Hasegawa. "Multi-Layer People Detection using 2D Range Data," *Proc. IEEE Int. Conf. on Robotics and Automation: Workshop on People Detection and Tracking*, 2009.

[12] S. Gidel, P. Checchin, C. Blanc, T. Chateau, and L. Trassoudaine, "Pedestrian detection method using a multilayer laserscanner: Application in urban environment," *Proc. Int. Conf. on Intelligent Robots and Systems (IROS)*, 2008, pp.173-178.

[13] L. Spinello , K. Arras, R. Triebel and R. Siegwart, "A Layered Approach to People Detection in 3D Range Data," *Proc. AAAI Conf. on Artificial Intelligence (AAAI)*, 2010.

[14] M. Ruhnke, B. Steder, G. Grisetti, W. Burgard, "Unsupervised Learning of 3D Object Models from Partial Views," *Proc. IEEE Int. Conf. on Robotics and Automation (ICRA)*, 2009.

[15] F. Chen, G. M. Brown, and M. Song, "Overview of three-dimensional shape measurement using optical methods," *Opt. Eng.*, Vol. 39, No. 10, 2000, pp. 10-22.

[16] K. H. Strobl, E. Mair, T. Bodenmüller, S. Kielhöfer, W. Sepp, M. Suppa, D. Burschka, G. Hirzinger, "The self-referenced DLR 3D-modeler," *Proc. Int. Conf. on Intelligent Robots and Systems (IROS)*, 2009, pp. 21-28.

[17] R. Sagawa, K. Nishino, K. Ikeuchi, "Adaptively Merging Large-Scale Range Data with Reflectance Properties," *IEEE Trans. on Pattern Analysis and Machine Intelligence*, vol. 27, no. 3, 2005, pp. 392-405.